

# Investigation to Assess Wind Effects on tall Structures by Computational Fluid Dynamics

G Naga Sulochana<sup>1</sup>, J Vara Prasad<sup>2</sup>, M.S.Anantha Venkatesh<sup>3</sup>, N Venkata Hussain Reddy<sup>4</sup>

<sup>1,4</sup>M. Tech Student, <sup>2,3</sup>Assistant Professor

<sup>1,2,3,4</sup>Department of Civil Engineering, AVR & SVR College of Engineering and Technology, Nandyal, Andhra Pradesh, India

## ABSTRACT

The tall building is the most dominating symbol of the cities and a human made marvel that defies gravity by reaching to clouds. The development of high strength concrete, higher grade steel, new construction techniques and advanced computational technique has resulted in the emergence of a new generation of tall structures that are flexible, low in damping, slender and light in weight. These types of flexible structures are very sensitive to dynamic wind loads and adversely affect the serviceability and occupant comfort. This project presents the results using Computational Fluid Dynamics Technique using Gambit & Fluent software on square and rectangular building models with an acceptance ratio of 1:1:7 & 1:1.5:7. The wind force on the models is evaluated from force records obtained from software under Computational Fluid Dynamics Technique using Gambit & Fluent for normal wind directions in a sub-urban terrain conditions for category A. The same rectangle building analyzed manually by IS 875 Part 3: 1987. The value obtained from this are compared with software results. The further study is made for the design and calculation of Gust Response Factor.

**Keywords :** Windward, Leeward, Guest Response, Acceptance Ratio.

## I. INTRODUCTION

### Importance Of wind Analysis on Tall Structures:

Wind is air in motion relative to the surface of the earth. The primary cause of wind is traced to earth's rotation and differences in terrestrial radiation. The radiation effects are primarily responsible for convection either upwards or downwards. The wind generally blows horizontal to the ground at high wind speeds. Since vertical components of atmospheric motion are relatively small, the term 'wind' denotes almost exclusively the horizontal wind, vertical winds are always identified as such. The wind speeds are assessed with the aid of anemometers or anemographs which are installed at meteorological observatories at heights generally varying from 10 to 30 meters above ground.

Very strong winds (greater than 80 km/h) are generally associated with cyclonic storms, thunderstorms, dust storms or vigorous monsoons. A feature of the Cyclonic storms over the Indian area is that they rapidly weaken after crossing the coasts and move as depressions/lows in land. The influence of a severe storm after striking the coast does not, in general exceed about 60 kilometers, though sometimes, it may extend even up to 120 kilometers. Very short duration hurricanes of very high wind speeds called KalBaisaki or Norwesters occur fairly frequently during summer months over east India.

The liability of a building to high wind pressures depends not only upon the geographical location and proximity of other obstructions to air flow but also upon the characteristics of the structure itself

The effect of wind on the structure as a whole is determined by the combined action of external and internal pressures acting upon it. In all cases, the calculated wind loads act normal to the surface to which they apply.

The stability calculations as a whole shall be done considering the combined effect, as well as separate effects of imposed loads and wind loads on vertical surfaces, roofs and other part of the building above general roof level. Buildings shall also be designed with due attention to the effects of wind on the comfort of people inside and outside the building.

## II. METHODS AND MATERIAL

### 2. LITERATURE SURVEY

#### 2.1 Wind Characteristics:

##### Basic Wind Pressures:

Figure 1 gives basic wind speed map of India, as applicable to 10 m height above mean ground level for different zones of the country. Basic wind speed is based

on peak gust velocity averaged over a short time interval of about 3 seconds and corresponds to mean heights above ground level in an open terrain (Category 2). Basic wind speeds presented in Fig. 1 have been worked out for a 50 year return period. Basic wind speed for some important cities/towns.

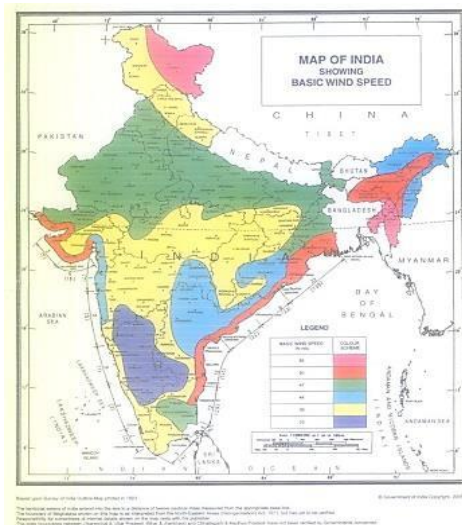


Figure 1. Basic Wind Speed

## 2.2 Gradient Wind Speed

The gradient wind is a balance of the Pressure Gradient Force, centrifugal and Coriolis. A geotropic wind becomes a gradient wind when the wind begins flowing through curved height contours. The curving motion introduces a centrifugal (outward fleeing) force. The centrifugal effect can be felt when turning through a curve in a car. You stay with the car but it feels like you are being pushed sideways.

## 2.3 Gust Factor

Only the method of calculating load along wind or drag load by using gust factor method is given in the code since methods for calculating load across-wind or other components are not fully matured for all types of structures. However, it is permissible for a designer to use gust factor method to calculate all components of load on a structure using any available theory. However, such a theory must take into account the random nature of atmospheric wind speed.

## 2.4 Turbulence characteristics

Gustiness occurs due to the velocity fluctuations present in the wind flow and this renders the forces exerted on the structure as dynamic forces. The degree of gustiness is given by standard deviation or RMS velocity value. The turbulent intensity can be obtained from SD and mean velocity and is given in equation.

$$I_u = \left( \frac{\sigma_u}{\bar{U}_z} \right) \text{ or } I_u = \left( \frac{1}{\ln(z/Z_0)} \right)$$

where

$I_u$  = turbulent intensity

$\sigma_u$  = standard deviation

$\bar{U}_z$  = mean velocity at height 'z'

$Z_0$  = terrain roughness length

Wind velocity has two components which are mean velocity that increases with height and turbulent velocity that remains same after gradient height. The variation of wind velocity with time has been illustrated in Fig. 3.3 and is given in equation

$$V_t = V + V'$$

Where,

$V_t$  = wind velocity at any given instant of time 't'

$V$  = average wind

$V'$  = wind gusts

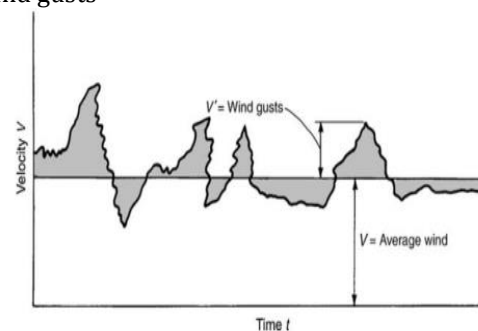


Figure 2. Variation of wind velocity with time

As wind pressures are proportional to the square and rectangle of velocities, with variation of mean Wind velocity, the mean pressures also fluctuate. The variation of pressure has been shown in Fig.2 and is given by:

$$P_t = P + P'$$

Where,

$P_t$  = pressure at any instant of time 't'

$P$  = Mean pressure

$P'$  = Gust pressure

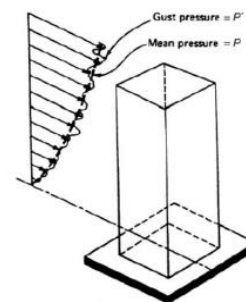


Figure 3. Schematic representation of mean and gust pressure at any instant of time 't' Along wind and across wind motions

Under the action of wind flow, structure experience aerodynamic forces that include the drag force and lift force. Drag (along-wind) force acting in the direction of the mean wind and the lift (across-wind) force acting perpendicular to that direction. The Along-wind motion primarily results from pressure fluctuations in the windward and the leeward faces, which generally follow

the fluctuations in the approach flow. The Across-wind motion is introduced by pressure fluctuations due to vortex shedding in the separated shear layers and wake flow field.

### 2.5 Wind force F

**Along Wind Load** - Along wind load on a structure on a strip area ( $A_e$ ) at any height ( $Z$ ) is given by:

$$F_S = C_f A_e P_z G$$

where

$F_S$  = along wind load on the structure at any height  $z$  corresponding to strip area  $A_e$

$C_f$  = force coefficient for the building,

$A_e$  = effective frontal area considered for the structure at height  $Z$ ,

$P_z$  = design pressure at height  $z$  due to hourly mean wind obtained as  $0.6 V_z^2$  ( $N/m^2$ )

### 3. Data Collection

#### Evaluation of wind force

Fig.10 (IS 875-3 Pg.51) shows the different faces of angles considered for the pressure measurement study. The chord length for each face is given as follows: Face A: 0- 10cm, Face B: 10- 25cm, Face C: 25- 35cm, Face D: 35- 50cm

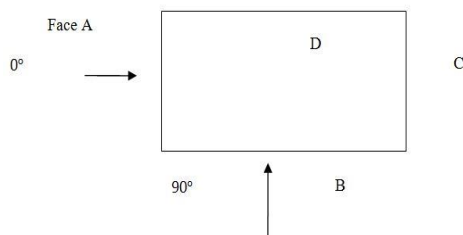


Figure 4. Forces Acting on Building

LEVEL S	Z/H	HEIGHT T in cm	RECTANGLE		SQUARE	
			Fx1987 (0°)	Fy1987 (90°)	Fx1987 (0°)	Fy1987 (90°)
1.000	0.1	7	447.81	904.42	298.50	904.40
2.000	0.2	14	596.18	1224.41	397.50	1224.40
3.000	0.3	21	686.04	1420.87	457.40	1420.90
4.000	0.5	35	1673.26	3473.53	1115.50	3473.50
5.000	0.7	49	1859.12	3874.31	1239.40	3874.30
6.000	0.8	56	983.51	2052.26	655.70	2052.30
7.000	0.9	63	1062.68	2256.65	708.50	2256.70
8.000	0.95	66.5	585.65	1196.70	390.40	1196.70
9.000	1	70	622.84	1310.19	415.20	1310.20

Table 7. Calculation of force as per IS-875(part-3) 1987 Provisions

Level	RECTANGLE		SQUARE	
	Leeward (90°)	Windward (0°)	Leeward (90°)	Windward (0°)
1.000	904.415	447.813	904.4	298.5
2.000	1224.411	596.178	1224.4	397.5
3.000	1420.865	686.036	1420.9	457.4
4.000	3473.529	1673.259	3473.5	1115.5
5.000	3874.313	1859.123	3874.3	1239.4
6.000	2052.260	983.512	2052.3	655.7
7.000	2256.651	1062.681	2256.7	708.5
8.000	1196.696	585.652	1196.7	390.4
9.000	1310.187	622.840	1310.2	415.2

Table 7. Calculation of force as per IS-875(part-3) 1987 Provisions

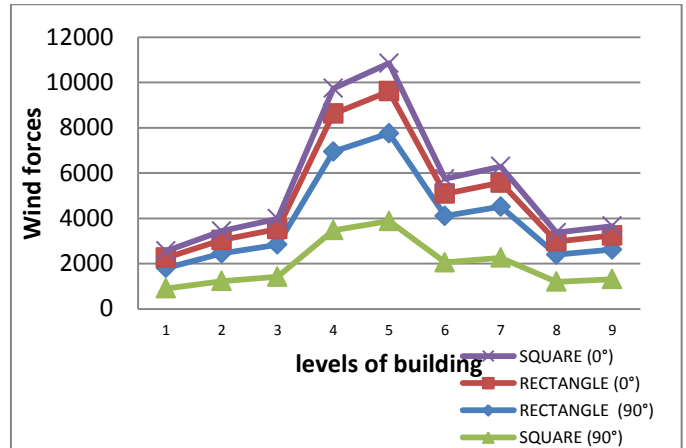
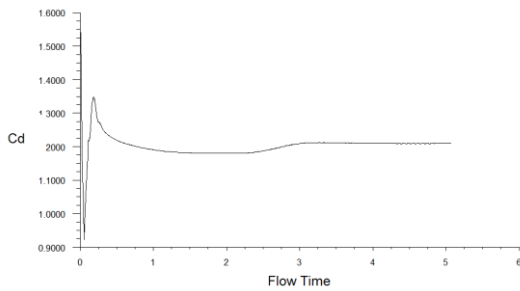


Figure 5. Forces for Manual Solutions

### III. RESULTS AND DISCUSSION

Unsteady numerical simulations have been carried out for a 1:2:5 rectangular building model under uniform wind flow condition using two types of turbulence models available in FLUENT 6.3 software: (i) Realizable k-ε turbulence model, which is single scale type turbulence model and (ii) DES turbulence model with Realizable k-ε option, which is multi-scale type hybrid turbulence model. For the evaluation of pressure coefficients and drag and lift force coefficients, the reference wind velocity is taken as 10 m/s (same as the uniform input wind velocity) and reference area of projected area, i.e. 0.1 m x 0.5 m. Unsteady simulations have been carried out until stabilized mean and standard deviation values of  $C_d$  and  $C_l$  are obtained with respect to time as shown in Fig.9 in IS 875-3 Pg.50 for Realizable k-ε turbulence model.

A MATLAB program has been developed for processing the numerically simulated  $C_p$  values to obtain distributions of mean  $C_p$  and standard deviation  $C_p$  values at 5 selected levels, viz. 0.05 m, 0.15 m, 0.25 m, 0.35 m, 0.45 m, respectively (correspond to  $z/H$  values of 0.1, 0.3, 0.5, 0.7, 0.9 ref. Level 1, Level 2, Level 3, Level 4, Level 5). Further mean  $C_d$  and standard deviation  $C_l$  values have been at these 5 levels and also for the overall building also. The following sections discuss some these results.



**Figure 6.** Variation of drag coefficient with time - Realizable k-ε turbulence model

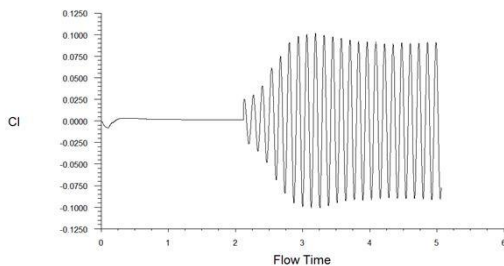


**Figure 7.** Variation of lift coefficient with time - Realizable k-ε turbulence model

### Velocity Vector Plots

Figs. 6 and 7 show the velocity vector plot on center vertical plane for Realizable k-ε case. It can be seen over the roof of building significant increase in wind velocity due to separation from the windward edge of the roof. Further in the wake region, i.e. rear side of the building, flow with recirculation is observed with wind in opposite direction along with vertical wind near to building rear side Fig.10 in IS 875-3 Pg.51 shows the velocity vector plot for DES case. Unlike for Realizable k-ε case, it can be seen multiple eddies in the wake region of the building, which is due to DES model can simulate multi-scale turbulence, i.e. eddies with different sizes.

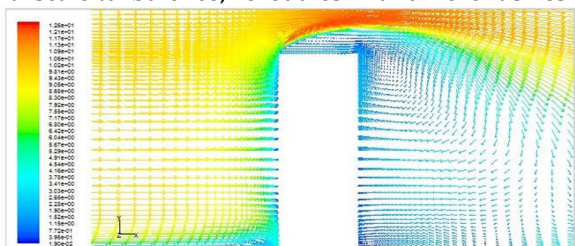


**Figure 8.** Velocity vector plot on center vertical plane - Realizable k-ε turbulence model

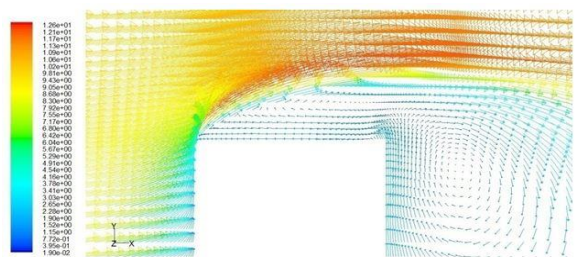


**Figure 9.** Close up view of velocity vector plot near building roof on center vertical plane- Realizable k-ε turbulence model

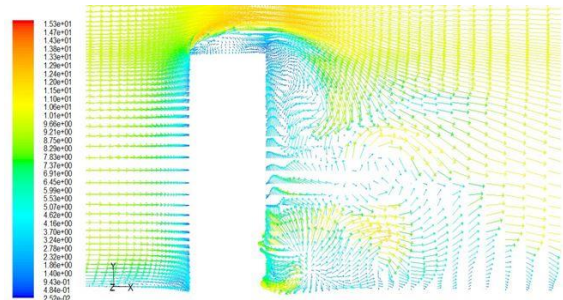


**Figure 10.** Velocity vector plot on center vertical plane - DES turbulence model

### Vorticity Contours

Vorticity is a measure of the rotation of a fluid element as it moves in the flow field and is defined as the curl of the velocity vector. It shows the vorticity contour plots in horizontal plane at Level 1, Level 3 and Level 5, respectively for Realizable k-ε turbulence model. It can be seen that the vortex shedding is predominant at Level 1 and as the height of the level increases, the vortex shedding phenomenon is observed to be affected. This is due to the wind flow from the top of the building into the wake region affecting the vortex shedding in the top region of the wake. Similarly Fig.9 in IS 875-3 Pg.50 show the vorticity contour plots in horizontal plane at Level 1, Level 3 and Level 5, respectively for DES turbulence model. Similar to Realizable k-ε predictions, the vortex shedding phenomenon is observed to be affected in the top region of the wake. However, DES predictions show vortex shedding with multiple eddies in the wake region.

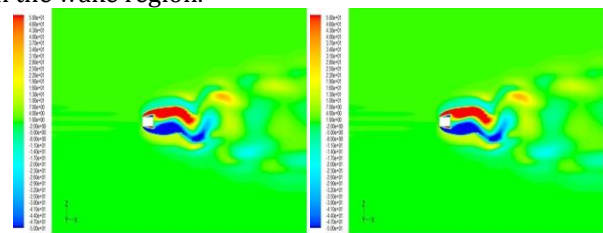


**Figure 11.** Vorticity Contour in horizontal plane at Level 1 - Realizable k-ε turbulence model

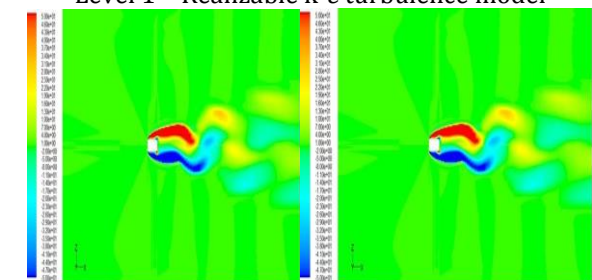


**Figure 12.** Vorticity Contour in horizontal plane at Level 3 - Realizable k-ε turbulence model

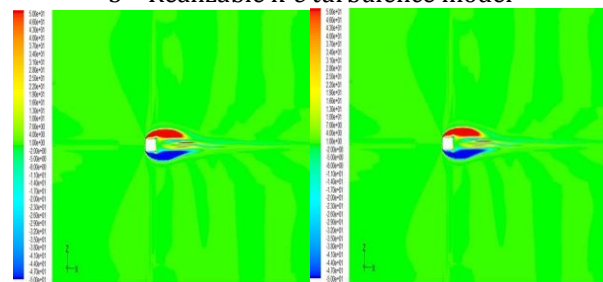


**Figure 13.** Vortices Contour in horizontal plane at Level 5 - Realizable k-ε turbulence model

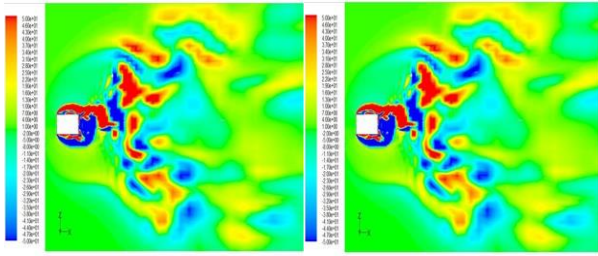


**Figure 14.** Vorticity Contour in horizontal plane at Level 1 – DES turbulence model

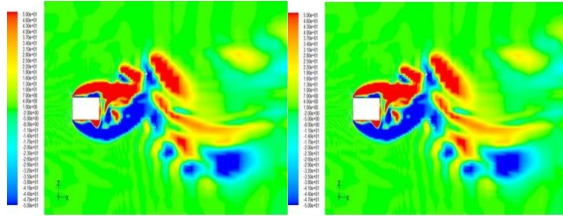


**Figure 15.** Vorticity Contour in horizontal plane at Level 3 – DES turbulence model

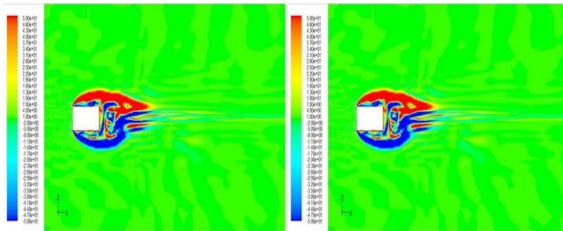


**Figure 16.** Vorticity Contour in horizontal plane at Level 5-DES turbulence model Mean Cp Distributions

Fig.10 in IS 875-3 Pg.51 show the mean  $C_p$  contour on the rectangular building obtained using Realizable  $k-\epsilon$  and DES turbulence models, respectively. It can be seen that on the front face, the mean  $C_p$  variation along the height is observed to be mostly uniform except at top and bottom regions, where the edge effects are expected. On the back face, the mean  $C_p$  values are observed to be negative, i.e suction pressure and their magnitudes are observed to be increasing with increase in height. However, on the side faces, difference in the mean  $C_p$  distributions is observed between the two turbulence models.

Further, mean  $C_p$  distributions along the circumference of the building at 5 levels, viz. Level 1, 2, 3, 4 and 5, have been shown in Fig.10 in IS 875-3 Pg.51 based on the Realizable  $k-\epsilon$  and DES turbulence models, respectively. It can be seen that for both the turbulence models, on the front face, the mean  $C_p$  values are almost same for Levels 2, 3 and 4, whereas at Levels 1 and 5, the mean  $C_p$  values are less. On the back face, in general, the mean  $C_p$  suction magnitudes are observed to be increasing with increase in height. On the side face, the mean  $C_p$  values are observed to be same for all the levels except for Level 1 in the case of Realizable  $k-\epsilon$  turbulence model. Fig.10 in IS 875-3 Pg.51 show the distribution of mean  $C_p$  along the circumference for levels 1, 3 and 5, respectively, to study the difference between the predictions of Realizable  $k-\epsilon$  and DES turbulence models. It can be seen that on the front face both the turbulence models predict almost same mean  $C_p$  values. However, the mean  $C_p$  suction magnitudes on the side and back faces are observed to be more in the case of DES

turbulence model than those in the case of Realizable  $k-\epsilon$  turbulence model. At Level 1, Realizable  $k-\epsilon$  turbulence model is observed to predict pressure recovery on the side faces from the windward edge. At Level 5, the mean  $C_p$  distribution along the side and back faces are observed to be nearly uniform based on both the turbulence models.

LEVELS	Z/H	HEIGHT in cm	RECTANGLE		SQUARE	
			Fx1987 (0°)	Fy1987 (90°)	Fx19 87 (0°)	Fy19 87 (90°)
1.000	0.1	7	438	904	428	890
2.000	0.2	14	586	1224	556	1100
3.000	0.3	21	676	1421	656	1311
4.000	0.5	35	1573	3474	1523	3364
5.000	0.7	49	1759	3874	1659	3764
6.000	0.8	56	974	2052	984	2042
7.000	0.9	63	963	2257	863	2157
8.000	0.95	66.5	566	1197	466	1297
9.000	1	70	310.	1310	428	890

**Table 7.** Calculation of force as per IS-875(part-3) 1987 Provisions

Level	RECTANGLE		SQUARE	
	Leeward (90°)	Windward (0°)	Leeward (90°)	Windward (0°)
1.000	900	438	890	428
2.000	1200	586	1100	556
3.000	1411	676	1311	656
4.000	3464	1573	3364	1523
5.000	3864	1759	3764	1659
6.000	2042	974	2042	984
7.000	2157	963	2157	863
8.000	1297	566	1297	466
9.000	632.84	310	890	428

**Table 7.** Calculation of force as per IS-875(part-3) 1987 Provisions

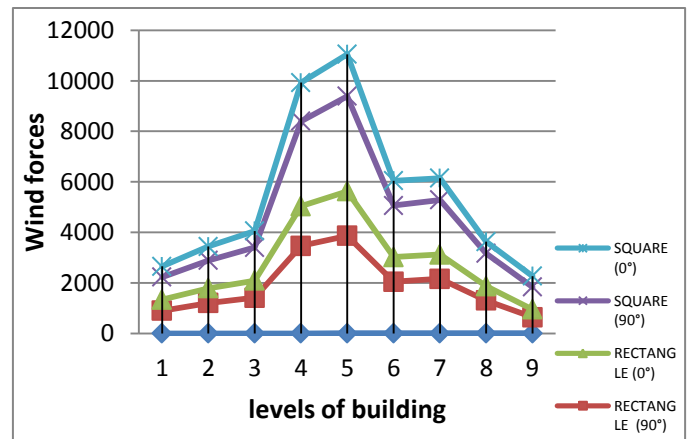


**Figure 17.** Forces for software solutions

Level	RECTANGLE				SQUARE			
	MANUAL		SOFTWARE		MANUAL		SOFTWARE	
	90°	0°	90°	0°	90°	0°	90°	0°
1.000	904.	447.	90	43	904.	298.	89	42
	42	81	0	8	41	54	0	8
2.000	1224	596.	12	58	122	397.	11	55

00	.41	18	00	6	4.41	45	00	6
3.0	1420	686.	14	67	142	457.	13	65
00	.87	04	11	6	0.87	36	11	6
4.0	3473	167	34	15	347	111	33	15
00	.53	3.26	64	73	3.53	5.51	64	23
5.0	3874	185	38	17	387	123	37	16
00	.31	9.12	64	59	4.31	9.42	64	59
6.0	2052	983.	20	97	205	655.	20	98
00	.26	51	42	4	2.26	67	42	4
7.0	2256	106	21	96	225	708.	21	86
00	.65	2.68	57	3	6.65	45	57	3
8.0	1196	585.	12	56	119	390.	12	46
00	.70	65	97	6	6.70	43	97	6
9.0	1310	622.	63	31	131	415.	63	31
00	.19	84	3	0	0.19	23	3	0

**Table 7.** Comparison of force for both manual and software solutions

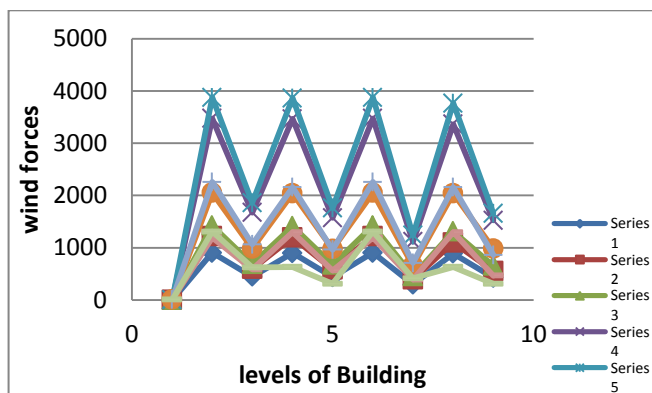


**Figure 18.** Comparison of force for both manual and software solutions

#### IV. CONCLUSION

Mean force value for  $0^\circ$  for Level 5 is always higher than all the other levels due to greater area of projection and edge effect at the ground level. For all other levels, values are almost same with draft code and IS: 875 (part-3) 1987 which indicates that these values are mostly governed by buffeting characteristics of approaching wind flow.

Mean force value for  $0^\circ$  for Level 5 is always higher than all the other levels due to greater area of projection and edge effect at the ground level. For all other levels, values are greater than with draft code and IS: 875 (part-3) 1987 of 0.2 ratio which indicates that these values are not governed by buffeting characteristics of approaching wind flow. Standard deviation of force coefficients shows decrease in value with height which shows that these parameters depend on the decrease in turbulence intensity with height. The mean value of drag and lift coefficients obtained from IS: 875 are which is in good agreement with code values for  $0^\circ$

but for  $90^\circ$ , these values are differing this is due to Wave Effect.

The manual value of force obtained from IS 875 Part 3. 3874.31 for  $90^\circ$  it is the drag coefficient and 904.42 for  $90^\circ$  of rectangle and 3874.31 for  $90^\circ$  it is the drag coefficient and 904.41 for  $90^\circ$  of square where as software value of force obtained from IS 875 Part 3. 3864 for  $90^\circ$  it is the drag coefficient and 900 for  $90^\circ$  of rectangle and 3764 for  $90^\circ$  it is the drag coefficient and 890 for  $90^\circ$  of square with Gambit and Fuent. This variation is due to vertex shedding at all levels. Manual values and values from software are almost similar to each other Gambit and fluent give best results for wind analysis. There was a variation of forces according to shapes of tall buildings so leeward and windward forces mainly depend on the shape of the model

#### V. REFERENCES

- [1] Alexandre Luis Braun and Armando Miguel Awruch, 2009. Aerodynamic and aeroelastic analyses on the CAARC standard tall building model using numerical simulation. *Computers and Structures*, 87, 564–581
- [2] Huang M.F., HLau I.W., Chan C.M., Kwok K.C.S. and G.Li, 2011. A hybrid RANS and kinematic simulation of wind load effects on full-scale tall buildings. *Journal Wind Eng. Ind. Aerodyn*, 99, 1126–1138.
- [3] Shenghong Huanga, Lib Q.S. and Shengli Xua, 2007. Numerical evaluation of wind effects on a tall steel building by CFD. *Journal of Constructional Steel Research*, 63, 612–627.
- [4] Claudio Mannini, Ante Soda and Gunter Schewe, 2011. Numerical investigation on the three-dimensional unsteady flow past a 5:1 rectangular cylinder. *Journal Wind Eng. Ind. Aerodyn*, 99, 469–482.
- [5] S. M. Fraser and C. Carey, 1990. Numerical and experimental analysis of flow around isolated and shielded cubes. *Appl. Math. Modelling*, 14, 588-597.
- [6] Bosch G. and Rodi W., 1998. Simulation of vortex shedding past a square cylinder with different turbulence models. *International Journal for Numerical Methods in Fluids*. 28, 601–616.
- [7] Kimura I. and Hosoda T., 2003. A non-linear k-ε model with realizability for prediction of flows around bluff bodies. *International Journal for Numerical methods in fluids*. 42, 813–837.
- [8] Shilpa G., Harikrishna p., Santhi A.S., Ramesh Babu G., 2014. Evaluation of Aerodynamic Pressure and Force coefficients for a 1:2:5Rectangular Building Model under Uniform Flow Condition in Wind Tunnel. *Proceedings of the International Conference on Advances in Sustainability of Materials and Environment, Nagercoil*. 10-11, 72-82.
- [9] IS: 875 (Part3)-1987.Code of practice for design loads (other than earthquake) for buildings and structures.